PTEN oxidation by mitochondrial ROS activates PI3K/AKT/mTOR pathway and induces mTOR-mediated autophagy during muscle differentiation

Jin-Hwan Kim[1, *], Tae Gyu Choi[1, *], Ngoc Ngo Yen Nguyen[2], Minh Nam Nguyen[1], Yong Hwa Jo[1], Abel Matondo[2], Michael P. Murphy[3], Insug Kang[2], Joungmok Kim[4], Joohun Ha[2] and Sung Soo Kim[1, †]

[1] Department of Biochemistry and Molecular Biology, School of Medicine, Kyung Hee University, 26 Kyungheedae-ro, Dongdaemun-gu, Seoul 02447, Republic of Korea

[2] Department of Biomedical Science, Graduate School, Kyung Hee University, 26 Kyungheedae-ro, Dongdaemun-gu, Seoul 02447, Republic of Korea

[3] MRC Mitochondrial Biology Unit, Hills Road, Cambridge CB2 0XY, UK

[4] Department of Oral Biochemistry and Molecular Biology , School of Dentistry, Kyung Hee University, 26 Kyungheedae-ro, Dongdaemun-gu, Seoul 02447, Republic of Korea

[*] These authors contributed equally to this work.

[†] To whom correspondence should be addressed at:
Sung Soo Kim, MD, PhD
Department of Biochemistry and Molecular Biology, School of Medicine, Kyung Hee University, 26 Kyungheedae-ro, Dongdaemun-gu, Seoul 02447, Republic of Korea.
Tel: 82-2-961-0524; Fax: 82-2-959-8168; E-mail: sgskim@khu.ac.kr.

Running title: PTEN oxidation by mtROS in muscle differentiation

Keyword: mitochondrial ROS, PTEN oxidation, mTORC1, autophagy, muscle differentiation

Abstract

Skeletal muscle differentiation is a crucial process controlling muscle development and homeostasis. Mitochondrial reactive oxygen species (mtROS), which are recently considered as critical cell signaling intermediates, rapidly increase during the muscle differentiation. However, it has not yet been elucidated how they control myogenic signaling. Autophagy, a lysosome-mediated degradation pathway, is importantly recognized for intracellular remodeling of cellular organelles during muscle differentiation. Here, we demonstrated that the mtROS are required for myogenic autophagy by stimulating PI3K/AKT/mTOR cascade. Activation of mTOR subsequently induced autophagic signaling via ULK1 phosphrylation at S317 to prompt muscle differentiation, whereas MitoQ or rapamycin treatment impaired the ULK1 phosphrylation. Conclusively, we propose a novel regulatory paradigm that mtROS are crucially required to initiate autophagic reconstruction of cellular organization through mTOR activation in muscle differentiation.

Introduction

Skeletal muscle differentiation is a highly coordinated sequential program to generate mature muscle fibers. The muscle differentiation proceeds through cell cycle withdrawal of myoblasts and increase in expression of muscle specific genes, leading to fusion of myoblasts into multinucleate myofibers [1].

In the muscle differentiation, phosphatidylinositol 3 kinase (PI3K)/Akt pathway is a crucial signaling cascade, which is mainly stimulated via insulin-like growth factors (IGFs) [2, 3]. A key repressor of this signaling, phosphatase and tensin homology deleted on chromosome 10 (PTEN), is a lipid phosphatase that dephosphorylates phosphatidylinositol-3,4,5-trisphosphate (PIP3) to phosphatidylinositol 4,5-bisphosphate (PIP2), thereby controlling the activity of PI3K/Akt signaling pathway [4, 5]. Enzymatic PTEN activity can be altered by post-translational regulation, including phosphorylation and oxidation [6]. Phosphorylation of PTEN prevents its recruitment to the plasma membrane and subsequently decreases its catalytic activity [7]. PTEN activity is also suppressed via oxidation of the essential C124 and the formation of a disulfide with C71 by H_2O_2 [8]. The elevated level of ROS exhibits activation of the PI3K/Akt signaling [9].

Mammalian target of rapamycin (mTOR) is well characterized as a serine/threonine kinase, which participates in a wide spectrum of cellular processes, including cell growth, proliferation, differentiation, survival, autophagy, and metabolism [10]. mTOR complex 1 (mTORC1) has emerged as a principal regulator of skeletal muscle differentiation [11]. It forms two different complexes, mTORC1 and mTORC2, that are dynamically assembled and cross-regulated with their modulators such as raptor, rictor, and LST8 via inter- and intra-complex loops [12, 13]. mTORC1 activates ribosomal protein kinase S6 kinase (S6K) and the eukaryotic translation initiation factor 4E (eIF4E)-binding proteins (4E-BPs) to regulate protein translation [14-16]. mTORC2 phosphorylates Akt, PKCs and serum- and glucocorticoid-induced protein kinases (SGKs), and regulates cell survival and actin cytoskeleton reorganization [11, 17].

Autophagy is a conserved catabolic process that degrades cellular components in lysosome [18]. Generally, the active mTORC1 interacts with the uncoordinated-51 (unc-51)-like kinase 1 (ULK1), and then directly phosphorylates ATG13L and ULK1 subunits at serine 258 (S258) and serine 757 (S757), respectively, to repress ULK1 kinase activity under nutrient-enriched condition [19, 20]. Subsequently, it sequesters ULK1/ATG13/FIP200 complex to prevent autophagy induction [21, 22]. Conversely, under nutrient-deprived condition, mTORC1 is dissociated from ULK1 complex, and then ULK1 is phosphorylated at serine 317 (S317) and serine 777 (S777) by AMP-activated protein kinase (AMPK) for autophagy initiation [23, 24]. However, it has not been explored whether mTOR is implicated in autophagy initiation to reconstruct intracellular organization for muscle differentiation

process which occurs under the nutrient-enriched condition.

In this study, we provide evidences that mitochondrial reactive oxygen species (mtROS) induce PTEN oxidation to stimulate PI3K/Akt/mTOR signaling pathway and thus promote autophagy which is required for skeletal muscle differentiation and regeneration.

Results

Mitochondrial ROS are increased during muscle differentiation

To examine the roles of mitochondria-generated ROS in the process of muscle differentiation, we first observed that myotube formation and myosin heavy chain (MHC) expression level were gradually increased up to 5 days after differentiation induction of C2C12 cells. Expression level of SOD2 was also elevated without change in SOD1 expression (Figure 1A), indicating that mtROS was upregulated during muscle differentiation. To further investigate the role of mtROS, we treated C2C12 cells with a mitochondria-targeted antioxidant, MitoQ, under differentiation medium (DM) condition. MitoQ significantly suppressed myotube formation and MHC expression as well as SOD2 expression in a dose-dependent manner (Figure 1B). A confocal microscopy analysis showed that MitoSOX intensity indicating mitochondrial superoxide ($O_2^{\cdot -}$) was also dramatically increased during differentiation, compared to proliferation medium (PM) condition, whereas mitochondrial $O_2^{\cdot -}$ level was reduced by MitoQ (Figure 1C). Next, we examined whether mtROS-derived cytosolic hydrogen peroxide (H_2O_2) regulates muscle differentiation. It is well known that galactose oxidase (GO) in the presence of D-galactose (GA) produces H_2O_2 in culture medium, which rapidly enters the cytosol [25]. Treatment of GA alone did not affect muscle differentiation and H_2O_2 production. Co-treatment of GA and GO enhanced myotube formation, MHC expression (Figure 1D) and intracellular H_2O_2 production (Figure 1E), compared to non-treatment in DM. Importantly, it was able to restore muscle differentiation with increased H_2O_2 production even in the presence of MitoQ.

Mitochondria-derived H_2O_2 regulates PTEN oxidation and activity during muscle differentiation

Previous studies have described that PTEN is inactivated via oxidation by H_2O_2, and its inactivation contributes to enhancing PI3K/AKT signaling [26-28]. Thus, we investigated whether PTEN was oxidized by H_2O_2 dismutated from mitochondrial $O_2^{\cdot -}$ by SOD2 during muscle differentiation. Indeed, oxidized PTEN (lower band) was gradually elevated without any changes in phosphorylated and total PTEN levels during 5 days of differentiation (Figure 2A). Consistently, PTEN activity was attenuated (Figure 2B). MitoQ dose-dependently decreased the oxidized level of PTEN with concomitant restoration of PTEN activity (Figure 2C and D). As expected, the co-treatment of GA and GO elevated PTEN oxidation level and reduced its activity even in the presence of MitoQ. Treatment of GA alone did not show any effect on PTEN oxidation and activity (Figure 2E and F).

PI3K/AKT/mTOR pathway is activated by mitochondrial ROS during muscle differentiation

PI3K/AKT/mTOR signaling pathway has an important role in muscle differentiation [29, 30]. Thus, we first tested whether the signaling cascade was activated during muscle differentiation. The PI3K downstream signaling molecules, such as PDK1, AKT, mTOR, p70S6K, and 4E-BP1, were gradually activated in differentiating myoblasts up to 5 days (Figure 3A). However, the mitochondria-targeted antioxidant, MitoQ, markedly diminished their phosphorylation levels (Figure 3B). To further investigate whether intracellular H_2O_2 affected PI3K/AKT/mTOR signaling, we treated differentiating myoblasts with GA and GO. As expected, the co-treatment further stimulated the phosphorylation of PI3K downstream molecules, and recovered the phosphorylation even in the presence of MitoQ (Figure 3C).

Silencing of PTEN enhances muscle differentiation and AKT phosphorylation

To further determine the role of PTEN, we investigated whether depletion of PTEN stimulated muscle differentiation. PTEN expression was interfered by its specific siRNA. The PTEN knockdown itself led to enhanced AKT phosphorylation in PM (Figure 4A). PTEN knockdowned cells exhibited further induction of myotube formation and MHC expression in DM, compared to scramble siRNA-transfected cells (Figure 4B). Consistent with PTEN knockdown, the chemical inhibition of PTEN activity using SF1670 stimulated MHC expression and AKT phosphorylation in a dose dependent manner (Figure 4C).

Mitochondrial ROS are required for mTOR activation to stimulate muscle differentiation

It is well-established that mTOR stimulates skeletal muscle differentiation [31]. Consistently, we found that MitoQ and mTOR inhibitor rapamycin suppressed p70S6K phosphorylation and MHC expression (Figure 5A). Therefore, we further investigated the interplay between mtROS and mTOR. The co-treatment of GA and GO did not rescue the myotube formation, p70S6K phosphorylation and MHC expression in presence of rapamycin (Figure 5B). Intriguingly, the rapamycin treatment did not influence the intracellular H_2O_2 level, similarly to non-treated condition. In addition, exogenous H_2O_2 by co-treatment of GA and GO did not restore MHC expression under the presence of rapamycin (Figure 5C).

mTOR activates autophagy during muscle differentiation

Muscle differentiation process requires the degradation of cellular components (autophagy) to remodel cellular organization for muscle fiber formation [32, 33]. The autophagy protects against apoptosis during myoblast differentiation [34, 35]. Thus, we thought that mTOR might induce autophagy under differentiation condition. We first observed autophagosome formation during muscle differentiation. LC3 puncta (green and red dot) formation was increased during muscle differentiation, but MitoQ or rapamycin completely attenuated LC3 puncta formation. As expected, bafilomycin and chloroquine, which suppress vacuolar-type H^+-ATPase and autolysosome formation, respectively [36, 37], highly increased the formation of LC3 puncta (Figure 6A and 6B). The inactivated mTORC1 by knockdown of raptor or mTOR decreased phosphorylations of p70S6K (Figure 6C) and impaired myotube formation (Figure 6D). Furthermore, the inhibition of mTORC1 did not restore MHC expression and LC3-II conversion even after co-treatment with GA and GO (Figure 6E and Figure 6F).

ULK1 phosphorylation is essential for autophagy initiation during muscle differentiation

It is well known that mTOR inhibits autophagy via unc-51 like kinase 1 (ULK1) phosphorylation at serine 757 (S757) in nutrient-enriched condition. In contrast, AMPK increases ULK1 phosphorylation at serine 317 (S317) to activate autophagy-initiation complex ULK1-Atg13-focal adhesion kinase family-interacting protein of 200 kDa (FIP200) under deprived condition [38, 39]. Therefore, it is important to understand whether mTOR stimulates ULK1 phosphorylation (S317) for the initiation of autophagy during muscle differentiation. Interestingly, ULK1 phosphorylation was increased at both S757 and S317 up to 5 days of differentiation (Figure 7A) without AMPK activation (data not shown), while MitoQ attenuated ULK1 phosphorylation at these sites in a dose-dependent manner (Figure 7B). Furthermore, the co-treatment of GA and GO also stimulated ULK1 phosphorylations even in the presence of MitoQ (Figure 7C). Rapamycin decreased ULK1 phosphorylation at both sites (Figure 7D), but the co-treatment of GA and GO did not restore ULK1 phosphorylation under rapamycin treatment (Figure 7E). To further investigate whether active mTOR (S2448) really phosphorylates ULK1 at S317 to induce autophagy, we performed co-immunoprecipitation. As the result, the active mTOR (S2448) interacted with phosphorylated ULK1 at the both sites of S757 and S317 in muscle differentiation. MitoQ or rapamycin disrupted the protein interactions (Figure 7F).

Increased mitochondrial ROS stimulate expressions of autophagy-related proteins (atgs) via mTOR activation during muscle differentiation

It was well known that autophagy process needs induction of autophagy-related proteins (atgs) to form autopahgosome [40]. We investigated atg protein expression levels such as atg3, 5, 7, and 12 as well as LC3 (atg8) conversion during muscle differentiation. The expression levels of atg proteins were gradually increased during differentiation process up to 5 days. Atg12-5 conjugated form, which is known to be essential for isolation of phagophore [41], was also increased (Figure 8A). MitoQ dose-dependently suppressed the expressions of atg proteins (Figure 8B), but co-treatment of GA and GO partially restored their expressions even in the presence of MitoQ (Figure 8C). The rapamycin treatment decreased Atg12-5 conjugation as well as Atg protein expressions (Figure 8D), but the Atg protein expressions and Atg12-5 conjugation were not restored even in the co-treatment of GA and GO (Figure 8E).

PTEN oxidation and mTOR activation are required for muscle regeneration

Muscle regeneration process is regulated by PI3K/Akt/mTOR signaling [42, 43]. Previous studies also described that PTEN inhibition and reactive oxygen species (ROS) are required for muscle regeneration and wound healing response [44, 45]. Thus, we injected cardiotoxin (CTX), which induced skeletal muscle necrosis [46], into the left tibialis anterior (TA) muscle. The results showed that muscle damage (white wound) was increased in the left TA muscle during 4 days after CTX injection, and then the recovery was gradually observed for the next 8 days. The PBS-injected right TA muscle did not show any change (Figure 9A). PTEN oxidation level was gradually increased without any change in total and phosphorylated PTEN level (Figure 9B). SOD2 expression level was also elevated during the same period of time. The downstream of PI3K/AKT/mTOR signaling molecules such as p70S6K and 4EBP1 were significantly activated after CTX injection (Figure 9C). ULK1 phosphorylations at S317 and S757 were also upregulated as well as the levels of Atg proteins during the TA muscle regeneration (Figure 9D).

Discussion

Here, we first reported that the drastic increase of mtROS stimulates PI3K/AKT/mTOR pathway through PTEN oxidative inactivation, and mTOR activation leads to autophagy initiation via ULK1 phosphorylation at Serine 317 during skeletal muscle differentiation. In addition, the elimination of mtROS by mitochondria-targeted antioxidant, MitoQ, attenuates the downstream signaling of mTOR, and ultimately blocks the myogenic autophagy.

Many studies have clearly shown that high level of ROS initiates cellular damage [47, 48]. However, it has also been proposed that physiologically low level of ROS serves as signaling molecules [49-51]. The intracellular ROS are recognized to be essential molecules for myogenesis [52, 53]. The preferential mitochondrial origin of ROS is further substantiated [54]. Also, we reported that gradual increase of mtROS is required for muscle differentiation [55]. In the current study, we firmly validated that mitochondrial $O_2^{\cdot-}$ stimulates muscle differentiation after dismutated to H_2O_2. To corroborate this result, we exogenously generated intracellular H_2O_2 by co-treatment of D-galactose and galactose oxidase. The expression level of SOD2 (a marker of mitochondrial $O_2^{\cdot-}$), but not SOD1 (a marker of cytosolic $O_2^{\cdot-}$), was also increased in differentiating myoblasts along with the elevation of mitochondrial $O_2^{\cdot-}$ level. The results showed that intracellular H_2O_2, which is dismutated from mitochondrial $O_2^{\cdot-}$ by MnSOD, is a key signaling molecule for muscle differentiation. Consistently, it was previously reported that the elevation of mitochondrial $O_2^{\cdot-}$ levels is required in adipocyte [56, 57], dendritic cell [58], keratinocyte differentiation [59].

PI3K regulates intracellular signal transduction pathways for numerous biological processes via interaction of diverse ligands with their receptors [60]. In case of muscle differentiation, insulin-like growth factors (IGFs) especially activate PI3K and its downstream Akt/mTOR signaling [61, 62]. PTEN inhibits the activation of downstream signaling, including Akt/mTOR, by catalyzing the conversion of PIP3 to PIP2 [63]. The PTEN activity can be post-transcriptionally inactivated via its reversible oxidative inactivation [64], resulting in activation of the PI3K/Akt cascade [8, 9]. We found that the gradual elevation of mtROS increasingly provokes PTEN oxidative inactivation, by which the PI3K/AKT signaling pathway is gradually activated for several days until muscle differentiation is terminated. In addition, MitoQ completely prevents PTEN oxidative inactivation. In agreement with previous studies [65-67], the chemical inhibition of PTEN or knockdown using its specific siRNA facilitates the myoblast differentiation. Collectively, we strongly assert that mtROS-imposed PTEN oxidation is essential to stimulate the PI3K/AKT/mTOR signaling and thus induce muscle differentiation.

Autophagy, a lysosome-mediated degradation pathway for recycling organelles and protein aggregates, is recognized to facilitate cell differentiation and development [68-70]. The complex

process begins at the phagophore assembly site (PAS) where proteins of the ULK1 complex, which is composed of ULK1, ATG13, FIP200 and ATG101, assemble to initiate autophagosome formation [71]. Under nutrient-enriched condition, mTOR directly phosphorylates ULK1 at S757, and thereby prevents ULK1 interaction with AMPK. In contrast, activated AMPK under nutrient-deprived condition phosphorylates ULK1 at S317 and S777 for initiating autophagy [22, 23]. Consequently, much of the current understanding of mTOR is limited in the context of inhibitory effects on autophagy in nutrient-enriched condition. However, myoblast differentiation requires autophagy to facilitate the elimination of pre-existing structures and promote cellular remodeling [72], indicating that the basic autophagy mechanism underlying muscle differentiation is completely different. In our results, mTOR activity was elevated to amplify autophagic process during muscle differentiation. Consistently, rapamycin or mTOR knockdown attenuated autophagy induction via inhibition of ULK1 phosphorylations at the both sites of S317 and S757. Furthermore, MitoQ-induced mTOR inactivation impaired the ULK1 phosphorylations (S317 and S757) and subsequent autophagy induction in muscle differentiation. Additionally, phosphorylation of ULK1 at S757 was increased by mTOR during muscle differentiation, which was diminished by MitoQ and rapamycin. Also, we showed that the active mTOR (S2448) interacts with phosphorylated ULK1 at both sites of S317 and S757 during muscle differentiation. Intriguingly, we also found that AMPK, a well-known autophagy inducer, is not activated during muscle differentiation (data not shown). Thus, we could exclude the possibility that AMPK phosphorylated ULK1 at S317 during muscle differentiation. From these results, we concluded that the active mTOR can simultaneously phosphorylate ULK1 at anti-autophagic S757 and pro-autophagic S317 and S777 sites during muscle differentiation, despite the fact that these phosphorylations lie on the antagonistic relation. This simultaneous dual phosphorylation of ULK1 at anti-autophagic S757 and pro-autophagic S317 and S777 was never reported before. More interestingly, phosphorylation of ULK1 at S757 could not block autophagy, when ULK1 was phosphorylated at S317 and S777, indicating that its pro-autophagic phosphorylation is predominant during muscle differentiation. It is accordingly possible that the activated mTOR induces autophagic reorganization of cellular components, which leads to the subsequent achievement of differentiated muscle fiber. In this context, our current study gives insight to new understanding that mTOR is inseparable from the autophagic induction, irrespectively of AMPK activation in muscle differentiation. At present, another co-regulator in myogenic autophagy remain to be sought out. It is therefore valuable to be further studied how mTOR induces ULK1 phosphorylation to initiate autophagy during myogenesis.

In summary, we first found that increased mitochondrial ROS are strongly involved in PTEN oxidative inactivation for enhancing PI3K/AKT/mTOR signaling activity. We also showed that mTOR activity induces myogenesis-specific autophagy by phosphorylating ULK1 at S317 without

involvement of AMPK during muscle differentiation.

Materials and Methods

Cell culture

C2C12 mouse myoblast cells were maintained in Dulbeco Modified Eagle's Medium (DMEM) supplemented with 10 % (v/v) fetal bovine serum, 100 U/ml of penicillin and 100 µg/ml streptomycin (proliferation medium, PM). C2C12 cells were induced to differentiate by replacing them in DMEM containing 2 % (v/v) horse serum, 100 U/ml of penicillin, and 100 µg/ml streptomycin (differentiation medium, DM). Full differentiation was achieved after 5 days in DM. Mouse embryonic fibroblast cells (MEF) were grown in DMEM supplemented with 10 % (v/v) fetal bovine serum, 100 U/ml of penicillin and 100 µg/ml streptomycin.

Reagents

Mito-Q was acquired from Dr. Micheal P Murpy. Mito-Tempol, bafilomycin A1, chloroquine, rapamycin, D-galactose, and galactose oxidase were purchased from Sigma Aldrich (St Louis, MO, USA). Torin 1 was purchased from Tocris (Bristol, UK). SF1670, LY294002, PLX4720, and AZD5363 were purchased from Sellekchemcals

Small interference RNA

The siPTEN was acquired from Cell Signaling (MA, USA). The siRNAs for mTOR and Raptor were taken from Sigma Aldrich (MO, USA). The siRNAs (400 nM / 60 mm dish) were transfected into C2C12 cells using Lipofectamine 2000 (Invitrogen, CA) for 48 hours. To evaluate the efficiency of siRNAs interference, the levels of PTEN, Raptor, and mTOR proteins were monitored by Western blot. Non-silencing control siRNA from cell signaling (MA, USA) was used as a control.

Intracellular H_2O_2 measurement

To quantify intracellular H_2O_2 level, cells were lysed with lysis buffer (120 mM KCl, 3 mM HEPES free acid, pH 7.2, 1 mM EGTA, and 0.3 % BSA). These lysates were added to each microplate well and pre-warmed at 37 °C for 10 minutes. Then, the reaction was started by adding 30 µg (50 ul) of cell lysate re-suspended in 50 µl of reaction buffer including 100 µM Amplex Red and 0.01 U/ml HRP. After 30 minutes, the absorbance of the reaction mixtures was measured at 560 nm using a microplate reader (Bio-Rad, Hercules, CA). A standard curve was prepared by addition of

known amounts of hydrogen peroxide.

Measurement of PTEN redox state and activity

Cells were harvested and washed twice with PBS, and resuspended in cell lysis buffer (1 % SDS, 10 % glycerol, 32 mM Tris-Cl, pH 6.8). Protein samples were subjected to SDS-PAGE under non-reducing conditions. The separated proteins were then transferred onto PDVF membrane and immunoblotted with an anti-PTEN antibody. The samples for PTEN phosphatase activity assay were prepared according to manufacturer protocol (Echelon Bioscience, UT USA).

Fusion assay (fusion index)

C2C12 cells were seeded in 60 mm dishes, cultivated in DM for 5 days, and stained with hematoxylin and eosin (H&E) staining. The fusion index (percentage of nuclei within myotubes and mononucleated cells) was determined using a microscope (Nikon, Tokyo, Japan). The total number of nuclei and myotubes was counted in 5 random fields (100 total nuclei) per each condition. A myotube was defined by the presence of at least three nuclei within a continuous cell membrane. Proliferating cells were used as a control.

Immunoprecipitation

Cells were lysed with lysis buffer (50 mM Tris-Cl, pH 7.4, 0.1 % NP40, and 150 mM NaCl) containing protease inhibitors and phosphatase inhibitors. For immunoprecipitation, the indicated antibody was coupled with protein A/G plus agarose bead (Santa Cruz, Dallas, TX) in 5 % bovine serum albumin (BSA) in TBST (20 mM Tris-Cl, pH 8.0, 170 mM NaCl, and 0.05 % Tween-20) for 2 hours. This immune complex was added to the cell lysates (500 μg) and incubated 4 °C for overnight. The resulting beads were washed with TBST five times before analysis.

Confocal microscopy observation

For mitochondrial ROS determination, C2C12 cells were stained using mitochondrial $O_2.^-$ indicator Mito-SOX (2 μM) for 30 minutes. After 2 times washing with 1X PBS, Mito-SOX intensity was observed at 510 nm. To quantify RFP (mcherry)-GFP-LC3-positive cells, C2C12 cells expressing GFP-LC3 were plated onto glass coverslips. After 5 days of differentiation in DM, the cells were fixed with 4 % paraformaldehyde for 30 minutes and rinsed with PBS twice. Cells were visualized at

488 nm under a confocal microscope (Carl Zeiss, Oberkochen, Germany). RFP (mcherry)-GFP-LC3-positive cells were randomly chosen in five different confocal microscopy images. Cells showing more than five strong GFP-positive dots were counted as RFP-GFP-LC3 positive dots. Total number of cells on images was determined by nuclei staining with DAPI (4', 6-diamidino-2-phenylindole).

Muscle injury.

The mouse left tibialis anterior (TA) muscle was injured by cardiotoxin (CTX) injection. Before the procedure, the mice were anesthetized. TA muscles were injected with 50 μl of 10 mM CTX solution in 0.9 % NaCl [73]. CTX-injured muscles were dissected on day 0 and the 1st, 2nd, 3rd, 4th, 6th, and 8th day following. The left TA muscles of non-injured mice were used as a control. Immediately after isolation, the muscles were frozen in liquid nitrogen and preserved at -80 °C. These tissues were homogenated and lysed with lysis buffer (50 mM Tris-Cl, pH 7.4, 0.1 % NP40, and 150 mM NaCl) containing protease and phosphatase inhibitors and analyzed by Western blot analysis. In every experiment, at least three animals were analyzed for each time point after CTX injury.

Western blot analysis

Cell lysates were collected in cell lysis buffer (1 % SDS, 10 % glycerol, 32 mM Tris-Cl, pH6.8) containing phosphatase and protease inhibitors, loaded on an SDS-PAGE gel, and electroblotted onto PVDF membrane. The primary antibodies were used as follows: MHC, β-actin, LC3 (Santa Cruz, Dallas, TX), SOD2 (Abfrontier, Seoul, Korea), PTEN, phospho-PTEN (Ser308/ Thr381/ Thr383), PDK1, phospho-PDK1 (Ser241), AKT, phospho-AKT (Ser473), mTOR, phospho-mTOR (Ser2481), phospho-mTOR (Ser2448), Raptor, p62/SQTM, p70S6K, phospho-p70S6K (Thr389), 4E-BP1, phospho-4E-BP1 (Thr37/46), ULK1, phospho-ULK1 (Ser317), phospho-ULK1 (Ser757), atg3, atg5, atg7, and atg12 (Cell Signaling). The primary antibodies were applied for overnight in 5% bovine serum albumin at 4 °C. The femto chemiluminescence kit (Thermo Scientific, Waltham, MA) was used for visualization of the signal. Immunoblots were analyzed using Image Lab (BioRad, Hercules, CA).

Statistical analysis

All data are representative of at least three individual experiments. Error bars were defined as standard error of the mean (SEM).

Acknowledgments

This study was supported by the National Research Foundation of Korea (NRF) grant funded by the Korea government (MEST) (No. 2011-0030072).

Author Contributions

J-HK and TGC conceived the study. J-HK, TGC and SSK supervised the study. J-HK, TGC, NNYN, MNN, YHJ and AAM performed the experiments. MPM provided materials and helpful discussion. IK and JH provided technical help and helpful discussion. J-HK, TGC, JK and SSK analyzed the data and wrote the manuscript.

Competing Financial Interests

The authors declare no competing financial interests.

References

1 Braun T, Gautel M. Transcriptional mechanisms regulating skeletal muscle differentiation, growth and homeostasis. *Nat Rev Mol Cell Biol* 2011; **12**:349-361.

2 Bodine SC, Stitt TN, Gonzalez M *et al.* Akt/mTOR pathway is a crucial regulator of skeletal muscle hypertrophy and can prevent muscle atrophy in vivo. *Nat Cell Biol* 2001; **3**:1014-1019.

3 Florini JR, Ewton DZ, Coolican SA. Growth hormone and the insulin-like growth factor system in myogenesis. *Endocr Rev* 1996; **17**:481-517.

4 Yamada KM, Araki M. Tumor suppressor PTEN: modulator of cell signaling, growth, migration and apoptosis. *J Cell Sci* 2001; **114**:2375-2382.

5 Sasaoka T, Wada T, Tsuneki H. Lipid phosphatases as a possible therapeutic target in cases of type 2 diabetes and obesity. *Pharmacol Ther* 2006; **112**:799-809.

6 Vazquez F, Grossman SR, Takahashi Y, Rokas MV, Nakamura N, Sellers WR. Phosphorylation of the PTEN tail acts as an inhibitory switch by preventing its recruitment into a protein complex. *J Biol Chem* 2001; **276**:48627-48630.

7 Das S, Dixon JE, Cho W. Membrane-binding and activation mechanism of PTEN. *Proc Natl Acad Sci U S A* 2003; **100**:7491-7496.

8 Kwon J, Lee SR, Yang KS *et al.* Reversible oxidation and inactivation of the tumor suppressor PTEN in cells stimulated with peptide growth factors. *Proc Natl Acad Sci U S A* 2004; **101**:16419-16424.

9 Kang KH, Lemke G, Kim JW. The PI3K-PTEN tug-of-war, oxidative stress and retinal degeneration. *Trends Mol Med* 2009; **15**:191-198.

10 Laplante M, Sabatini DM. mTOR signaling in growth control and disease. *Cell* 2012; **149**:274-293.

11 Ge Y, Chen J. Mammalian target of rapamycin (mTOR) signaling network in skeletal myogenesis. *J Biol Chem* 2012; **287**:43928-43935.

12 Jacinto E, Facchinetti V, Liu D *et al.* SIN1/MIP1 maintains rictor-mTOR complex integrity and regulates Akt phosphorylation and substrate specificity. *Cell* 2006; **127**:125-137.

13 Sarbassov DD, Ali SM, Kim DH *et al.* Rictor, a novel binding partner of mTOR, defines a rapamycin-insensitive and raptor-independent pathway that regulates the cytoskeleton. *Curr Biol* 2004; **14**:1296-1302.

14 Ma XM, Blenis J. Molecular mechanisms of mTOR-mediated translational control. *Nat Rev Mol Cell Biol* 2009; **10**:307-318.

15 Sengupta S, Peterson TR, Sabatini DM. Regulation of the mTOR complex 1 pathway by nutrients, growth factors, and stress. *Mol Cell* 2010; **40**:310-322.

16 Zoncu R, Efeyan A, Sabatini DM. mTOR: from growth signal integration to cancer, diabetes and ageing. *Nat Rev Mol Cell Biol* 2011; **12**:21-35.

17 Sarbassov DD, Guertin DA, Ali SM, Sabatini DM. Phosphorylation and regulation of Akt/PKB by the rictor-mTOR complex. *Science* 2005; **307**:1098-1101.

18 Kaur J, Debnath J. Autophagy at the crossroads of catabolism and anabolism. *Nat Rev Mol Cell Biol* 2015; **16**:461-472.

19 Kamada Y, Funakoshi T, Shintani T, Nagano K, Ohsumi M, Ohsumi Y. Tor-mediated induction of autophagy via an Apg1 protein kinase complex. *J Cell Biol* 2000; **150**:1507-1513.

20 Chan EY. mTORC1 phosphorylates the ULK1-mAtg13-FIP200 autophagy regulatory complex. *Sci Signal* 2009; **2**:pe51.

21 Hosokawa N, Hara T, Kaizuka T *et al.* Nutrient-dependent mTORC1 association with the ULK1-Atg13-FIP200 complex required for autophagy. *Mol Biol Cell* 2009; **20**:1981-1991.

22 Jung CH, Jun CB, Ro SH *et al.* ULK-Atg13-FIP200 complexes mediate mTOR signaling to the autophagy machinery. *Mol Biol Cell* 2009; **20**:1992-2003.

23 Kim J, Kundu M, Viollet B, Guan KL. AMPK and mTOR regulate autophagy through direct phosphorylation of Ulk1. *Nat Cell Biol* 2011; **13**:132-141.

24 Jung CH, Ro SH, Cao J, Otto NM, Kim DH. mTOR regulation of autophagy. *FEBS Lett* 2010; **584**:1287-1295.

25 Wang Y, DuBois JL, Hedman B, Hodgson KO, Stack TD. Catalytic galactose oxidase models: biomimetic Cu(II)-phenoxyl-radical reactivity. *Science* 1998; **279**:537-540.

26 Lee SR, Yang KS, Kwon J, Lee C, Jeong W, Rhee SG. Reversible inactivation of the tumor suppressor PTEN by H2O2. *J Biol Chem* 2002; **277**:20336-20342.

27 Connor KM, Subbaram S, Regan KJ *et al.* Mitochondrial H2O2 regulates the angiogenic phenotype via PTEN oxidation. *J Biol Chem* 2005; **280**:16916-16924.

28 Wu KL, Wu CA, Wu CW, Chan SH, Chang AY, Chan JY. Redox-sensitive oxidation and phosphorylation of PTEN contribute to enhanced activation of PI3K/Akt signaling in rostral ventrolateral medulla and neurogenic hypertension in spontaneously hypertensive rats. *Antioxid Redox Signal* 2013; **18**:36-50.

29 Crespo FL, Sobrado VR, Gomez L, Cervera AM, McCreath KJ. Mitochondrial reactive oxygen species mediate cardiomyocyte formation from embryonic stem cells in high glucose. *Stem Cells* 2010; **28**:1132-1142.

30 Hlobilkova A, Knillova J, Bartek J, Lukas J, Kolar Z. The mechanism of action of the tumour suppressor gene PTEN. *Biomed Pap Med Fac Univ Palacky Olomouc Czech Repub* 2003; **147**:19-25.

31 Erbay E, Park IH, Nuzzi PD, Schoenherr CJ, Chen J. IGF-II transcription in skeletal

myogenesis is controlled by mTOR and nutrients. *J Cell Biol* 2003; **163**:931-936.

32 Zembron-Lacny A, Krzywanski J, Ostapiuk-Karolczuk J, Kasperska A. Cell and molecular mechanisms of regeneration and reorganization of skeletal muscles. *Ortop Traumatol Rehabil* 2012; **14**:1-11.

33 Pizon V, Gerbal F, Diaz CC, Karsenti E. Microtubule-dependent transport and organization of sarcomeric myosin during skeletal muscle differentiation. *EMBO J* 2005; **24**:3781-3792.

34 McMillan EM, Quadrilatero J. Autophagy is required and protects against apoptosis during myoblast differentiation. *Biochem J* 2014; **462**:267-277.

35 Martinez-Lopez N, Athonvarangkul D, Sahu S *et al.* Autophagy in Myf5+ progenitors regulates energy and glucose homeostasis through control of brown fat and skeletal muscle development. *EMBO Rep* 2013; **14**:795-803.

36 Bowman EJ, Siebers A, Altendorf K. Bafilomycins: a class of inhibitors of membrane ATPases from microorganisms, animal cells, and plant cells. *Proc Natl Acad Sci U S A* 1988; **85**:7972-7976.

37 Mizushima N, Levine B, Cuervo AM, Klionsky DJ. Autophagy fights disease through cellular self-digestion. *Nature* 2008; **451**:1069-1075.

38 Inoki K. mTOR signaling in autophagy regulation in the kidney. *Semin Nephrol* 2014; **34**:2-8.

39 Dunlop EA, Tee AR. mTOR and autophagy: a dynamic relationship governed by nutrients and energy. *Semin Cell Dev Biol* 2014; **36**:121-129.

40 Otomo C, Metlagel Z, Takaesu G, Otomo T. Structure of the human ATG12~ATG5 conjugate required for LC3 lipidation in autophagy. *Nat Struct Mol Biol* 2013; **20**:59-66.

41 Fukuda M, Itoh T. Direct link between Atg protein and small GTPase Rab: Atg16L functions as a potential Rab33 effector in mammals. *Autophagy* 2008; **4**:824-826.

42 Li HY, Zhang QG, Chen JW, Chen SQ, Chen SY. The fibrotic role of phosphatidylinositol-3-kinase/Akt pathway in injured skeletal muscle after acute contusion. *Int J Sports Med* 2013; **34**:789-794.

43 Zhang P, Liang X, Shan T *et al.* mTOR is necessary for proper satellite cell activity and skeletal muscle regeneration. *Biochem Biophys Res Commun* 2015; **463**:102-108.

44 Hu Z, Wang H, Lee IH *et al.* PTEN inhibition improves muscle regeneration in mice fed a high-fat diet. *Diabetes* 2010; **59**:1312-1320.

45 Vasilaki A, Jackson MJ. Role of reactive oxygen species in the defective regeneration seen in aging muscle. *Free Radic Biol Med* 2013; **65**:317-323.

46 Ownby CL, Fletcher JE, Colberg TR. Cardiotoxin 1 from cobra (Naja naja atra) venom causes necrosis of skeletal muscle in vivo. *Toxicon* 1993; **31**:697-709.

47 Orrenius S, Gogvadze V, Zhivotovsky B. Mitochondrial oxidative stress: implications for cell

death. *Annu Rev Pharmacol Toxicol* 2007; **47**:143-183.

48 Circu ML, Aw TY. Reactive oxygen species, cellular redox systems, and apoptosis. *Free Radic Biol Med* 2010; **48**:749-762.

49 Finkel T. Signal transduction by reactive oxygen species. *J Cell Biol* 2011; **194**:7-15.

50 Choi TG, Lee J, Ha J, Kim SS. Apoptosis signal-regulating kinase 1 is an intracellular inducer of p38 MAPK-mediated myogenic signalling in cardiac myoblasts. *Biochim Biophys Acta* 2011; **1813**:1412-1421.

51 Schieber M, Chandel NS. ROS function in redox signaling and oxidative stress. *Curr Biol* 2014; **24**:R453-462.

52 Bakkar N, Guttridge DC. NF-kappaB signaling: a tale of two pathways in skeletal myogenesis. *Physiol Rev* 2010; **90**:495-511.

53 Lee J, Choi KJ, Lim MJ *et al.* Proto-oncogenic H-Ras, K-Ras, and N-Ras are involved in muscle differentiation via phosphatidylinositol 3-kinase. *Cell Res* 2010; **20**:919-934.

54 Remels AH, Langen RC, Schrauwen P, Schaart G, Schols AM, Gosker HR. Regulation of mitochondrial biogenesis during myogenesis. *Mol Cell Endocrinol* 2010; **315**:113-120.

55 Lee S, Tak E, Lee J *et al.* Mitochondrial H2O2 generated from electron transport chain complex I stimulates muscle differentiation. *Cell Res* 2011; **21**:817-834.

56 Wang W, Zhang Y, Lu W, Liu K. Mitochondrial reactive oxygen species regulate adipocyte differentiation of mesenchymal stem cells in hematopoietic stress induced by arabinosylcytosine. *PLoS One* 2015; **10**:e0120629.

57 Tormos KV, Anso E, Hamanaka RB *et al.* Mitochondrial complex III ROS regulate adipocyte differentiation. *Cell Metab* 2011; **14**:537-544.

58 Del Prete A, Zaccagnino P, Di Paola M *et al.* Role of mitochondria and reactive oxygen species in dendritic cell differentiation and functions. *Free Radic Biol Med* 2008; **44**:1443-1451.

59 Hamanaka RB, Glasauer A, Hoover P *et al.* Mitochondrial reactive oxygen species promote epidermal differentiation and hair follicle development. *Sci Signal* 2013; **6**:ra8.

60 Vanhaesebroeck B, Guillermet-Guibert J, Graupera M, Bilanges B. The emerging mechanisms of isoform-specific PI3K signalling. *Nat Rev Mol Cell Biol* 2010; **11**:329-341.

61 Shavlakadze T, Chai J, Maley K *et al.* A growth stimulus is needed for IGF-1 to induce skeletal muscle hypertrophy in vivo. *J Cell Sci* 2010; **123**:960-971.

62 Schiaffino S, Dyar KA, Ciciliot S, Blaauw B, Sandri M. Mechanisms regulating skeletal muscle growth and atrophy. *FEBS J* 2013; **280**:4294-4314.

63 Leevers SJ, Vanhaesebroeck B, Waterfield MD. Signalling through phosphoinositide 3-kinases: the lipids take centre stage. *Curr Opin Cell Biol* 1999; **11**:219-225.

64 Leslie NR, Bennett D, Lindsay YE, Stewart H, Gray A, Downes CP. Redox regulation of PI 3-

kinase signalling via inactivation of PTEN. *EMBO J* 2003; **22**:5501-5510.

65 Mandl A, Sarkes D, Carricaburu V, Jung V, Rameh L. Serum withdrawal-induced accumulation of phosphoinositide 3-kinase lipids in differentiating 3T3-L6 myoblasts: distinct roles for Ship2 and PTEN. *Mol Cell Biol* 2007; **27**:8098-8112.

66 Majmundar AJ, Skuli N, Mesquita RC *et al.* O(2) regulates skeletal muscle progenitor differentiation through phosphatidylinositol 3-kinase/AKT signaling. *Mol Cell Biol* 2012; **32**:36-49.

67 White ES, Atrasz RG, Hu B *et al.* Negative regulation of myofibroblast differentiation by PTEN (Phosphatase and Tensin Homolog Deleted on chromosome 10). *Am J Respir Crit Care Med* 2006; **173**:112-121.

68 Mizushima N, Komatsu M. Autophagy: renovation of cells and tissues. *Cell* 2011; **147**:728-741.

69 Boya P, Reggiori F, Codogno P. Emerging regulation and functions of autophagy. *Nat Cell Biol* 2013; **15**:713-720.

70 Wirawan E, Vanden Berghe T, Lippens S, Agostinis P, Vandenabeele P. Autophagy: for better or for worse. *Cell Res* 2012; **22**:43-61.

71 Lamb CA, Yoshimori T, Tooze SA. The autophagosome: origins unknown, biogenesis complex. *Nat Rev Mol Cell Biol* 2013; **14**:759-774.

72 Mizushima N, Levine B. Autophagy in mammalian development and differentiation. *Nat Cell Biol* 2010; **12**:823-830.

73 Czerwinska AM, Streminska W, Ciemerych MA, Grabowska I. Mouse gastrocnemius muscle regeneration after mechanical or cardiotoxin injury. *Folia Histochem Cytobiol* 2012; **50**:144-153.

Figure legends

Figure 1. Mitochondrial ROS are increased during muscle differentiation. (A) Morphological changes were observed during the progression of differentiation in DM for 5 days. Expressions of MHC, SOD1 and SOD2 were analyzed by Western blot using specific antibodies. (B) MitoQ (MQ) was treated with 125, 250 and 500 nM for 5 days. The protein levels of MHC, SOD1 and SOD2 at indicated days were analyzed by Western blot analysis. (C) Mitochondrial $O_2^{\cdot-}$ was stained with 1 μM MitoSOX and were observed by confocal microscope. (D) Cells were treated with 0.25 mM GA with or without 0.015 U/ml GO in DM for 5days. Under this condition, 250 nM MQ was treated from 2 days after induction of differentiation, and further incubated for 3 days. The expressions of MHC, SOD1 and SOD2 were analyzed by Western blot. (E) Under the same condition in Figure 1C, cells were stained with 2 μM Amplex Red, and the optical density (OD, at 560 nm) values for intracellular H_2O_2 were evaluated using microplate reader. β-actin was used as a loading control. The data shown represent the mean ± SE of three independent experiments.

Figure 2. Mitochondrial H_2O_2 regulates PTEN oxidation and activity during muscle differentiation. C2C12 cells were incubated in DM for 5 days and the medium was changed every day. (A) Proteins were resolved by non-reducing SDS-PAGE gel. The reduced (*upper band*) and oxidized (*lower band*) forms of PTEN protein, phosphor-PTEN (p-PTEN) and PTEN were analyzed by Western blot. (B) For PTEN activity assay, cells were harvested in indicated conditions. The PIP3-hydrolyzing activity of PTEN was determined and expressed by percentage, compared to PM. * $p <$ 0.05, compared to cells in PM. (C) C2C12 cells were treated with 125, 250, and 500 nM Mito-Q for 5 days, and the reduced and oxidized PTEN proteins were analyzed by Western blot. (D) Under the same condition in Figure 2C, the PTEN activity was determined at 450 nm and expressed by percentage. * $p < 0.05$, compared to cells in PM. $^{\#}$ $p < 0.05$, compared to cells in DM. (E) Cells were treated with 0.25 mM GA with or without 0.015 U/ml GO in DM for 5days. Under this condition, 250 nM MQ was treated from 2 days after induction of differentiation, and further incubated for 3 days. (F) Under the same condition in Figure 2E, the PTEN activity was determined at 450 nm and expressed by percentage. * $p < 0.05$, compared to cells in PM. $^{\#}$ $p < 0.05$, compared to cells treated with GA in DM. ¶ $p < 0.05$, compared to cells treated with GA and GO in DM. β-actin was used as a loading control. In graphs, the data shown represent the mean ± SE of three independent experiments.

Figure 3. PI3K/AKT/mTOR pathway activation by mitochondrial ROS during muscle differentiation. (A) C2C12 cells were cultured in DM for 5 days (*left panel*). Cells were treated with 250 nM MitoQ (MQ) or 100 μM mito-tempol (MT) for 5 days (*right panel*). (B) Cells were treated

with 0.25 mM GA with or without 0.015 U/ml GO in DM for 5days. Under this condition, 250 nM MQ was treated from 2 days after induction of differentiation, and further incubated for 3 days. Phospho-PDK1 at serine 241 (p-PDK1 S241), PDK1, phospho-AKT at serine473 (p-AKT S473), AKT, phospho-mTOR at serine 2448 (p-mTOR S2448), phospho-mTOR at serine 2481 (p-mTOR S2481), phospho-p70S6K at serine 371 (p-p70S6K S371), p70S6K, phospho-4E-BP1 at threonine 37 and 46 (p-4E-BP1 T37/46), 4E-BP1, and MHC were analyzed by Western blot. β-actin was used as a loading control.

Figure 4. Silencing of PTEN enhances muscle differentiation and AKT phosphorylation. (A) C2C12 cells were transfected with 100, 200 and 400 pM PTEN siRNA (si-PTEN) for 48 hours, and then PTEN expression and Akt activity and expression were evaluated by Western blot analysis. (B) After transfection with 100, 200 and 400 nM si-PTEN, the cells were further incubated in DM for 5 days. Then, morphological changes were observed. MHC expression, Akt activity and expression were assessed by Western blot analysis. (C) Cells were treated with 30 and 60 nM SF1670 in DM for 5 days. (D) Cells were treated with 0.25 mM GA with or without 0.015 U/ml GO in DM for 5days. Under this condition, 60 nM SF1670 was treated from 2 days after induction of differentiation, and further incubated for 3 days. β-actin was used as a loading control.

Figure 5. mitochondrial ROS-induced mTOR activation stimulates muscle differentiation. (A) C2C12 cells were treated with 500 nM MitoQ (MQ) or 250 pM rapamycin (Rapa) in DM for 5 days. The cells were harvested at 1, 3, and 5 days of differentiation. Indicated proteins were assessed by Western blot. (B) Cells were treated with 0.25 mM GA with or without 0.015 U/ml GO in DM for 5days. Under this condition, 250 pM MQ was treated from 2 days after induction of differentiation, and further incubated for 3 days. (C) cells were stained with 2 μM Amplex Red, and the OD values at 560 nm for intracellular H_2O_2 were evaluated using microplate reader. β-actin was used as a loading control.

Figure 6. Autopahgy induction by mTOR activation is essential for muscle differentiation. (A) C2C12 cells were transfected with mCherry-GFP LC3 for 48 hours, and then 500 nM MitoQ (MQ), 0.5 nM bafilomycin A1 (Baf), 2.5 μM chloroquine (CQ), and 0.5nM rapamycin (Rapa)were treated in DM for 5 days. The fluorescence was visualized by confocal microscopy. DAPI was used for nuclear staining. (B) Quantification of autophagosome flux was represented. LC3 puncta were calculated by counting GFP (green) and (mCherry) red dots in the mcherry-GFP LC3 transfected cells and expressed as a percentage of cell with LC3 dots (minimum five dots per cell). * $p < 0.05$, compared to cells in PM. $^{\#}$ $p < 0.05$, compared to cells in DM. (C) C2C12 cells were transfected with 400 nM si-

Raptor or si-mTOR for 48 hours, and then protein levels were assessed by Western blot. (D) fusion index was measured at 5 days after induction of differentiation. * $p < 0.05$, compared to cells in PM. $^{\#}$ $p < 0.05$, compared to cells in DM. (E) After 48-hour transfection with si-Raptor or si-mTOR, the cells were treated with 0.25 mM GA with or without 0.015 U/ml GO in DM for 5 days. Under this condition, 250 nM MQ was treated from 2 days after induction of differentiation, and further incubated for 3 days. β-actin was used as a loading control. the data shown represent the mean ± SE of three independent experiments.

Figure 7. mTOR phosphorylates ULK1 at serine 317 for autophagy initiation during muscle differentiation. (A) C2C12 cells were incubated in differentiation medium up to 5 days and were harvested every day. (B) Cells were incubated with 125, 250, and 500 nM MitoQ (MQ) for 5 days. MQ containing media were changed every day. (C) Cells were treated with 0.25 mM GA with or without 0.015 U/ml GO in DM for 5 days. Under this condition, 250 nM MQ was treated from 2 days after induction of differentiation, and further incubated for 3 days. (D) Cells were incubated with 125, 250, and 500 pM rapamycin (Rapa) for 5 days. (E) Cells were treated with 0.25 mM GA with or without 0.015 U/ml GO in DM for 5 days. Under this condition, 250 pM MQ was treated from 2 days after induction of differentiation, and further incubated for 3 days. The levels of phospho-ULK1 at serine 317 (pULK1 S317), phospho-ULK1 at serine 757 (pULK1 S757), and ULK1 were assessed by Western blot analysis. β-actin was used as a loading control.

Figure 8. Increased mitochondrial ROS stimulate expression of autophagy-related proteins (atgs) via mTOR activation during muscle differentiation (A) C2C12 cells were incubated in differentiation medium up to 5 days and were harvested every day. (B) Cells were incubated with 125, 250, and 500 nM MitoQ (MQ) for 5 days. MQ containing media were changed every day. (C) Cells were treated with 0.25 mM GA with or without 0.015 U/ml GO in DM for 5days. Under this condition, 250 nM MQ was treated from 2 days after induction of differentiation, and further incubated for 3 days. (D) Cells were incubated with 125, 250, and 500 pM rapamycin (Rapa) for 5 days. (E) Cells were treated with 0.25 mM GA with or without 0.015 U/ml GO in DM for 5days. Under this condition, 250 pM MQ was treated from 2 days after induction of differentiation, and further incubated for 3 days. The levels of atg3, atg5, atg7, atg12, atg5-atg12, and LC3 (LC3-I, upper; LC3-II, lower) were assessed by Western blot analysis. β-actin was used as a loading control.

Figure 9. PTEN oxidation and mTOR activation are generated for muscle regeneration in mouse model (A) Mouse left tibialis anterior (TA) muscle was injected with 50 μl (10 mM)

cardiotoxin (CTX). Mouse was sacrificed at indicated days after the injection (N = 5). (B) Mouse tibialis anterior (TA) muscle tissues were homogenated and analyzed by Western blot analysis. The oxidized and reduced PTEN were resolved by nonreducing SDS-PAGE. The levels of phospho-PTEN (pPTEN), PTEN, AKT, SOD2, and MHC proteins were analyzed by Western blot analysis. (C) CTX injected TA muscle tissues were homogenated and resolved by SDS-PAGE. The levels of phospho-AKT (pAKT S473), AKT, phospho-mTOR (pmTOR S2448), phospho-p70S6K (pp70S6K S371), p70S6K, phospho-4E-BP1 (p4E-BP1 T37/46), 4E-BP1 were determined by Western blot analysis. (D) The levels of phospho-ULK1 (pULK1 S757), phospho-ULK1 (pULK1 S757), ULK1, atg3, atg5, atg7, atg12, atg5-atg12, and LC3 were analyzed by Western blot analysis. β-actin was used as a loading control.

Figure 1

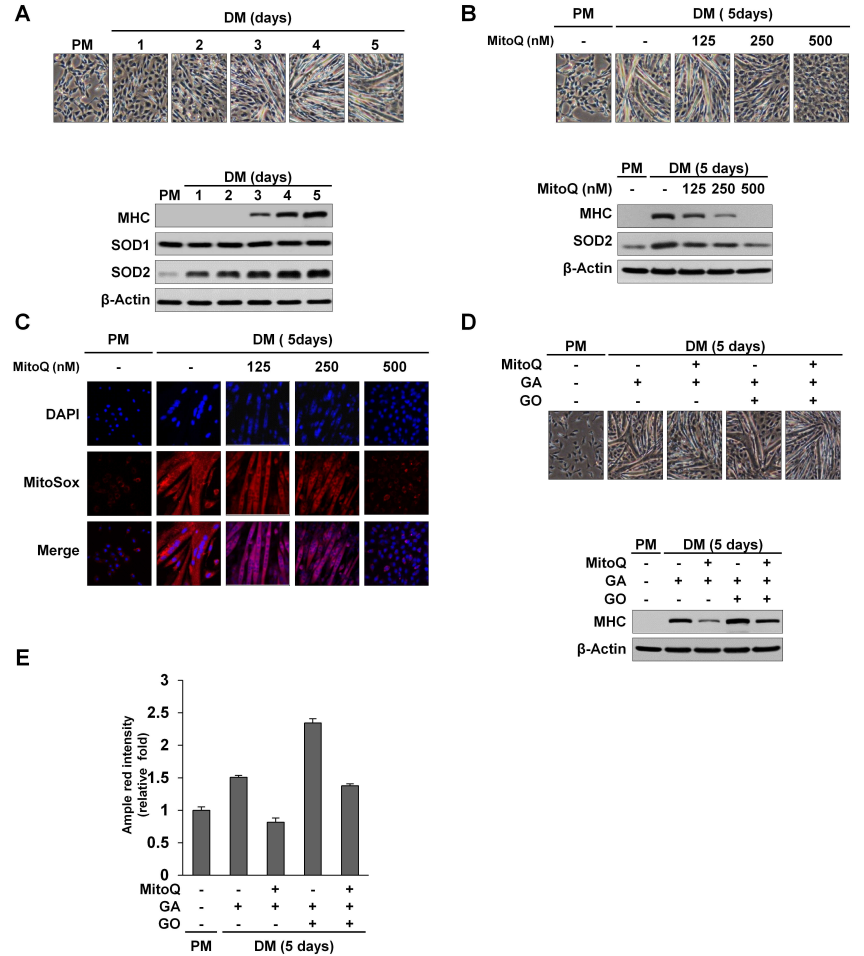
A
DM (days)
PM
1
2
3
4
5
DM (days)
PM 1 2 3 4 5
MHC
SOD1
SOD2
β-Actin
B
PM
DM (5days)
MitoQ (nM)
-
-
125
250
500
PM
DM (5 days)
MitoQ (nM)
- - 125 250 500
MHC
SOD2
β-Actin
C
PM
DM (5days)
MitoQ (nM)
-
-
125
250
500
DAPI
MitoSox
Merge
D
PM
DM (5 days)
MitoQ
GA
GO
PM
DM (5 days)
MitoQ
GA
GO
MHC
β-Actin
E
Ample red intensity (relative fold)
3
2.5
2
1.5
1
0.5
0
MitoQ
GA
GO
PM
DM (5 days)

Figure 2

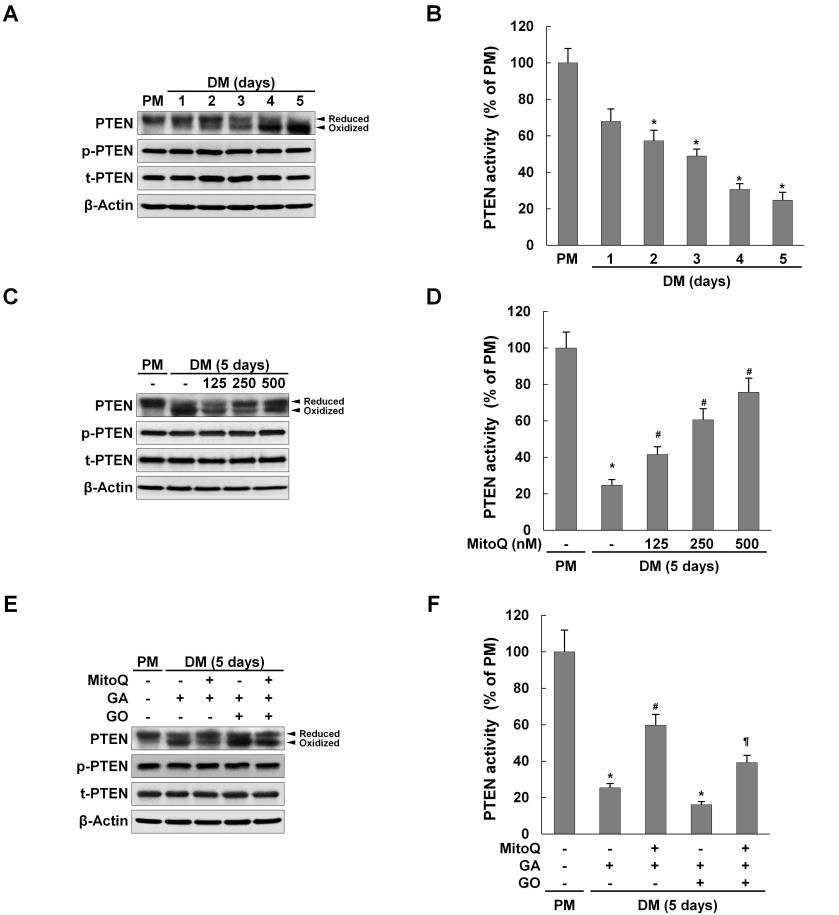
A
DM (days)
PM 1 2 3 4 5
PTEN
p-PTEN
t-PTEN
β-Actin
Reduced
Oxidized
B
PTEN activity (% of PM)
120
100
80
60
40
20
0
PM 1 2 3 4 5
DM (days)
C
PM DM (5 days)
- - 125 250 500
PTEN
p-PTEN
t-PTEN
β-Actin
Reduced
Oxidized
D
PTEN activity (% of PM)
MitoQ (nM) - - 125 250 500
PM DM (5 days)
E
PM DM (5 days)
MitoQ - - + - +
GA - + + + +
GO - - - + +
PTEN
p-PTEN
t-PTEN
β-Actin
Reduced
Oxidized
F
PTEN activity (% of PM)
MitoQ - - + - +
GA - + + + +
GO - - - + +
PM DM (5 days)

Figure 3

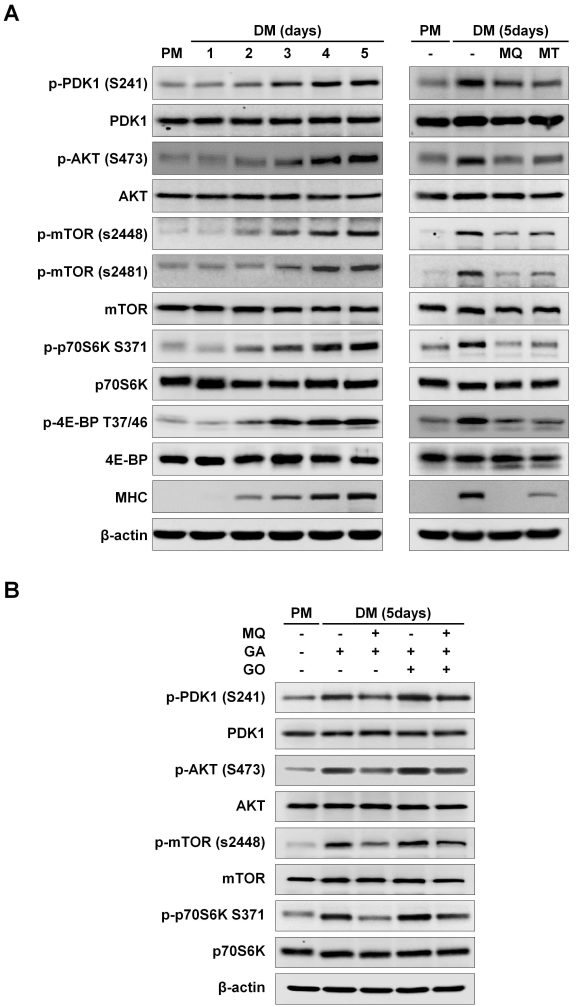
A
DM (days)
PM
1
2
3
4
5
PM
DM (5days)
-
-
MQ
MT
p-PDK1 (S241)
PDK1
p-AKT (S473)
AKT
p-mTOR (s2448)
p-mTOR (s2481)
mTOR
p-p70S6K S371
p70S6K
p-4E-BP T37/46
4E-BP
MHC
β-actin
B
PM
DM (5days)
MQ - - + - +
GA - + + + +
GO - - - + +
p-PDK1 (S241)
PDK1
p-AKT (S473)
AKT
p-mTOR (s2448)
mTOR
p-p70S6K S371
p70S6K
β-actin

Figure 4

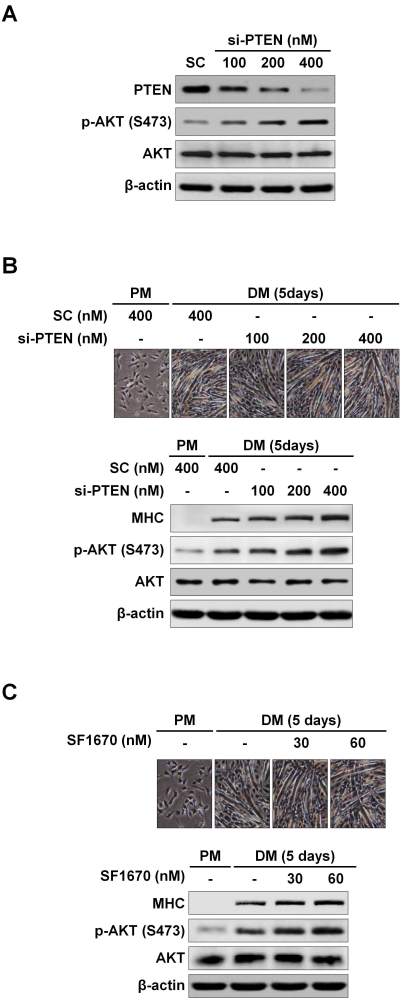
A
si-PTEN (nM)
SC
100
200
400
PTEN
p-AKT (S473)
AKT
β-actin
B
PM
DM (5days)
SC (nM)
400
400
-
-
-
si-PTEN (nM)
-
-
100
200
400
PM
DM (5days)
SC (nM)
400
400
-
-
-
si-PTEN (nM)
-
-
100
200
400
MHC
p-AKT (S473)
AKT
β-actin
C
PM
DM (5 days)
SF1670 (nM)
-
-
30
60
PM
DM (5 days)
SF1670 (nM)
-
-
30
60
MHC
p-AKT (S473)
AKT
β-actin

Figure 5

A

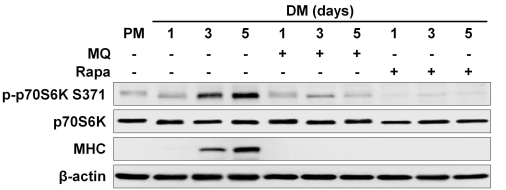
DM (days)
PM 1 3 5 1 3 5 1 3 5
MQ - - - - + + + - - -
Rapa - - - - - - - + + +
p-p70S6K S371
p70S6K
MHC
β-actin

B

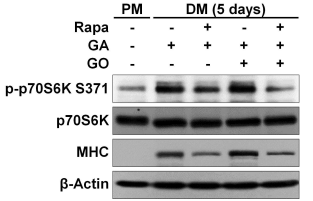
PM
DM (5 days)
Rapa - - + - +
GA - + + + +
GO - - - + +
p-p70S6K S371
p70S6K
MHC
β-Actin

C

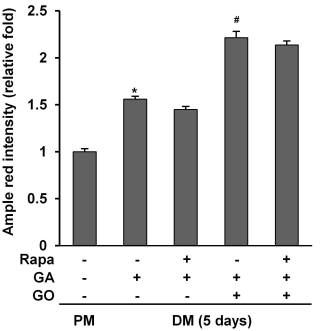
Ample red intensity (relative fold)
2.5
2
1.5
1
0.5
0
*
#
Rapa - - + - +
GA - + + + +
GO - - - + +
PM
DM (5 days)

Figure 6

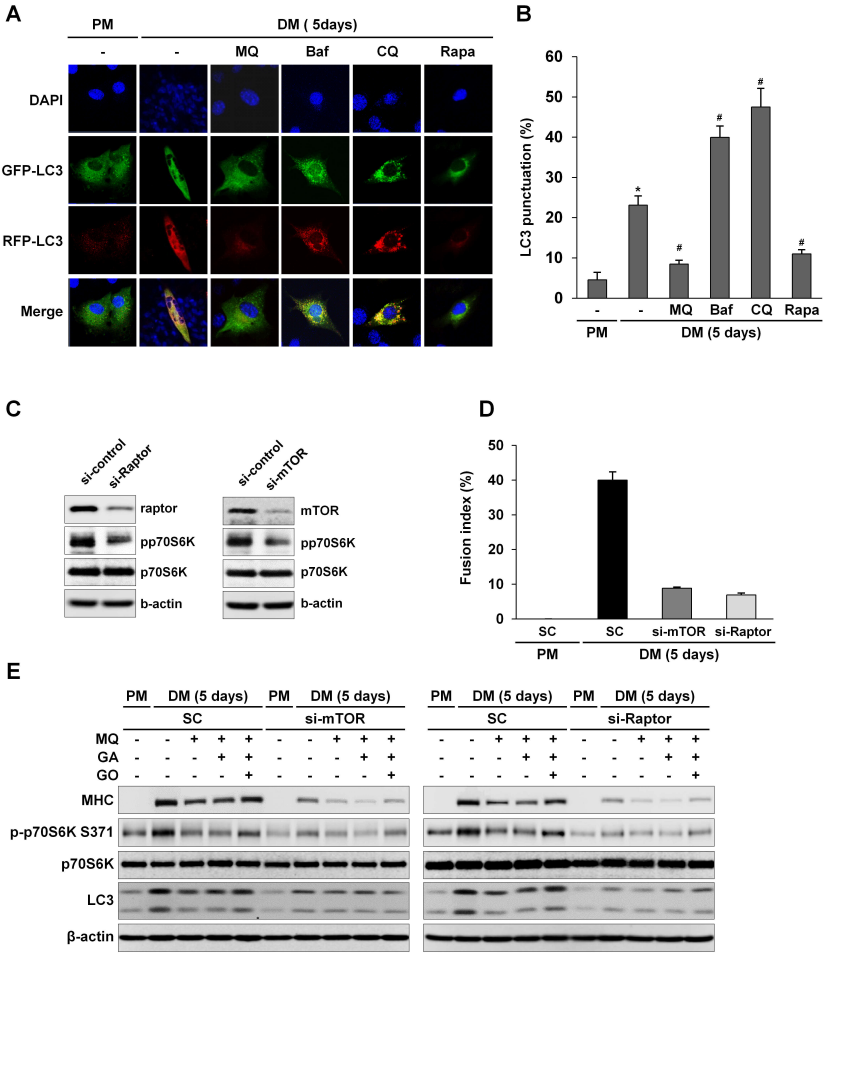
A
PM
DM (5days)
-
-
MQ
Baf
CQ
Rapa
DAPI
GFP-LC3
RFP-LC3
Merge
B
LC3 punctuation (%)
60
50
40
30
20
10
0
*
#
PM
DM (5 days)
C
si-control
si-Raptor
si-control
si-mTOR
raptor
mTOR
pp70S6K
p70S6K
b-actin
D
Fusion index (%)
50
40
30
20
10
0
SC
si-mTOR
si-Raptor
E
PM
DM (5 days)
SC
si-mTOR
si-Raptor
MQ
GA
GO
MHC
p-p70S6K S371
p70S6K
LC3
β-actin

Figure 7

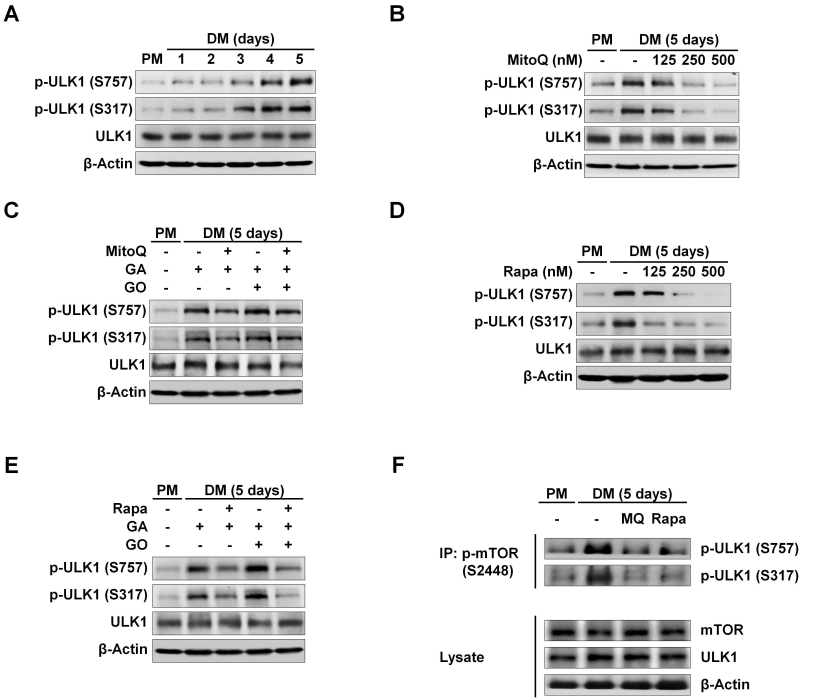
A
DM (days)
PM 1 2 3 4 5
p-ULK1 (S757)
p-ULK1 (S317)
ULK1
β-Actin
B
PM DM (5 days)
MitoQ (nM) - - 125 250 500
p-ULK1 (S757)
p-ULK1 (S317)
ULK1
β-Actin
C
PM DM (5 days)
MitoQ - - + - +
GA - + + + +
GO - - - + +
p-ULK1 (S757)
p-ULK1 (S317)
ULK1
β-Actin
D
PM DM (5 days)
Rapa (nM) - - 125 250 500
p-ULK1 (S757)
p-ULK1 (S317)
ULK1
β-Actin
E
PM DM (5 days)
Rapa - - + - +
GA - + + + +
GO - - - + +
p-ULK1 (S757)
p-ULK1 (S317)
ULK1
β-Actin
F
PM DM (5 days)
- - MQ Rapa
IP: p-mTOR (S2448)
p-ULK1 (S757)
p-ULK1 (S317)
Lysate
mTOR
ULK1
β-Actin

Figure 8

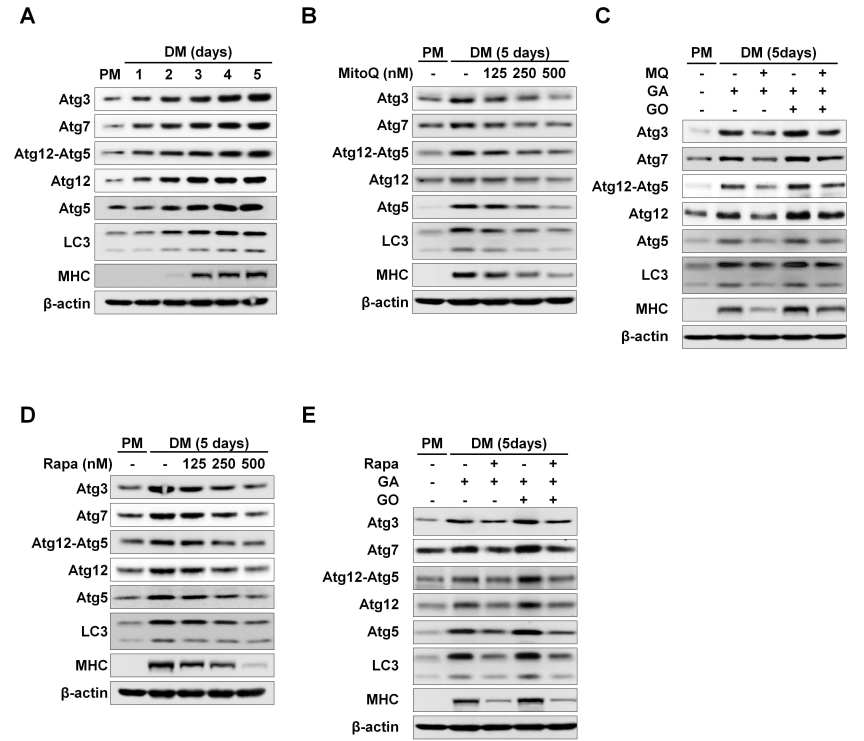
A
DM (days)
PM 1 2 3 4 5
Atg3
Atg7
Atg12-Atg5
Atg12
Atg5
LC3
MHC
β-actin
B
PM DM (5 days)
MitoQ (nM) - - 125 250 500
Atg3
Atg7
Atg12-Atg5
Atg12
Atg5
LC3
MHC
β-actin
C
PM DM (5days)
MQ - - + - +
GA - + + + +
GO - - - + +
Atg3
Atg7
Atg12-Atg5
Atg12
Atg5
LC3
MHC
β-actin
D
PM DM (5 days)
Rapa (nM) - - 125 250 500
Atg3
Atg7
Atg12-Atg5
Atg12
Atg5
LC3
MHC
β-actin
E
PM DM (5days)
Rapa - - + - +
GA - + + + +
GO - - - + +
Atg3
Atg7
Atg12-Atg5
Atg12
Atg5
LC3
MHC
β-actin

Figure 9

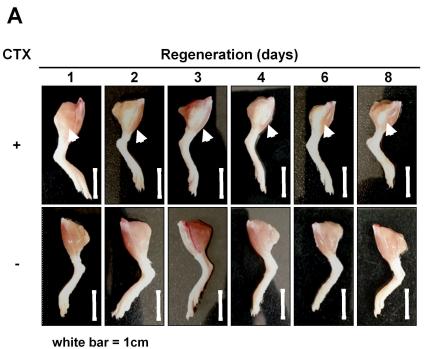
A
CTX
Regeneration (days)
1
2
3
4
6
8
+
-
white bar = 1cm

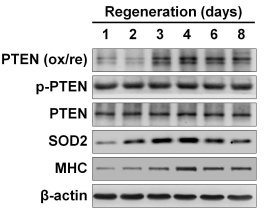
B
Regeneration (days)
1 2 3 4 6 8
PTEN (ox/re)
p-PTEN
PTEN
SOD2
MHC
β-actin

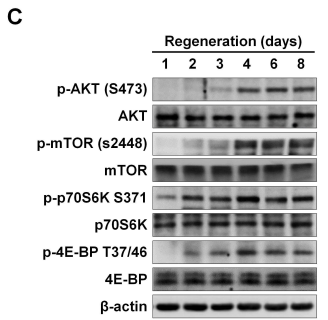
C
Regeneration (days)
1 2 3 4 6 8
p-AKT (S473)
AKT
p-mTOR (s2448)
mTOR
p-p70S6K S371
p70S6K
p-4E-BP T37/46
4E-BP
β-actin

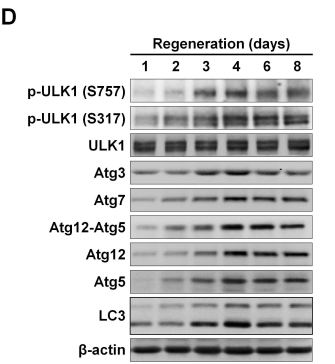
D
Regeneration (days)
1 2 3 4 6 8
p-ULK1 (S757)
p-ULK1 (S317)
ULK1
Atg3
Atg7
Atg12-Atg5
Atg12
Atg5
LC3
β-actin